

# Laboratory Evidence of Transient Pressure Surge in a Fluid-Filled Fracture as a Potential Driver of Remote Dynamic Earthquake Triggering

Yuesu Jin\*1, Nikolay Dyaur<sup>2</sup>, and Yingcai Zheng<sup>1</sup>

#### **Abstract**

Seismic waves carrying tiny perturbing stresses can trigger earthquakes in geothermal and volcanic regions. The underlying cause of this dynamic triggering is still not well understood. One leading hypothesis is that a sudden increase in the fluid-pore pressure in the fault zone is involved, but the exact physical mechanism is unclear. Here, we report experimental evidence in which a fluid-filled fracture was shown to be able to amplify the pressure of an incoming seismic wave. We built miniature pressure sensors and directly placed them inside a thin fluid-filled fracture to measure the fluid pressure during wave propagation. By varying the fracture aperture from 0.2 to 9.2 mm and sweeping the frequency from 12 to 70 Hz, we observed in the lab that the fluid pressure in the fracture could be amplified up to 25.2 times compared with the incident-wave amplitude. Because an increase of the fluid pressure in a fault can reduce the effective normal stress to allow the fault to slide, our observed transient pressure surge phenomenon may provide the mechanism for earthquake dynamic triggering.

Cite this article as Jin, Y., Dyaur, N., and Zheng, Y. (2021). Laboratory Evidence of Transient Pressure Surge in a Fluid-Filled Fracture as a Potential Driver of Remote Dynamic Earthquake Triggering. *The Seismic Record.* 1, 66–74, doi: 10.1785/0320210015.

#### Introduction

Earthquakes can be triggered by passing seismic waves—a phenomenon known as dynamic triggering. The underlying mechanism behind dynamic triggering is still not well understood (Hill *et al.*, 1993; Prejean *et al.*, 2004; Brodsky and van der Elst, 2014; Hill and Prejean, 2015; Cattania *et al.*, 2017; Li *et al.*, 2021). The stress amplitudes of the passing waves are very low (on the order of kPa). The triggered occurrences are often observed in geothermal or volcanic regions where fluids and fractures are abundant and ubiquitous. Furthermore, the triggering thresholds for these triggered events seem to be more sensitive to long-period incident waves than short-period waves of comparable amplitudes (Brodsky and Prejean, 2005; Hill and Prejean, 2015).

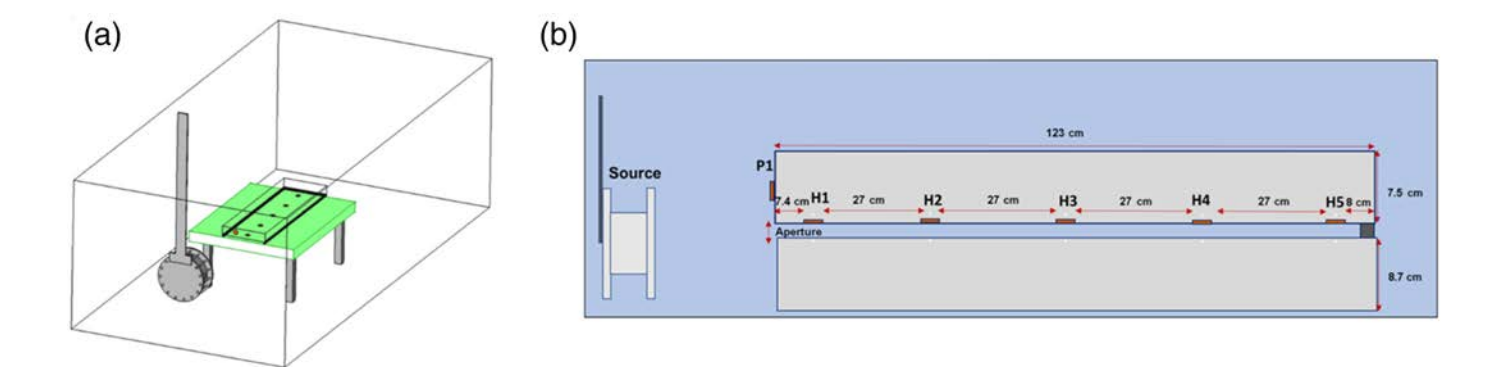
Two hypotheses have been proposed to explain the cause of dynamic triggering. The first one is the critical state hypothesis (e.g., Zoback and Zoback, 2002). It says that the crust is close to rupturing, and any stress perturbation, as small as the one imposed by a traveling seismic wave, could cause failures.

However, this explanation does not explain why these triggered phenomena have an affinity with fluids. It also does not explain the frequency dependence of the triggering and repeated triggering (Peng et al., 2011). The second hypothesis says that pore pressure may have increased locally to cause the dynamic triggering (Hill, 2008; Brodsky and van der Elst, 2014), but the mechanism is unknown. Recently, Zheng (2018) discovered a transient pressure surge (PS) phenomenon in numerical modeling of wave propagation using a 2D boundary element method. He found that when a seismic wave interacted with a fluid-filled fracture, the fluid pressure in the fracture could be

<sup>1.</sup> Department of Earth and Atmospheric Sciences, University of Houston, Houston, Texas, U.S.A., https://orcid.org/0000-0001-9179-8940 (YZ); 2. Schmidt Institute of Physics of the Earth, Russian Academy of Sciences, Moscow, Russian Federation, https://orcid.org/0000-0002-2842-9883 (ND)

<sup>\*</sup>Corresponding author: yjin6@central.uh.edu

<sup>© 2021.</sup> The Authors. This is an open access article distributed under the terms of the CC-BY license, which permits unrestricted use, distribution, and reproduction in any medium, provided the original work is properly cited.



amplified by 2–3 orders of magnitude compared with the incident-wave pressure. This amplification is a natural consequence of solving the wave equation in the fluid and solid media, and enforcing the fluid-solid boundary conditions at the millimeter scale. No other exotic mechanism needs to be invoked. It was suggested that the slow interface wave due to the two fluid-solid boundaries (Krauklis, 1962; Ferrazzini and Aki, 1987) was responsible for the pressure amplification. If the fluid pressure can be transiently amplified in a fracture, we also expect to see a local pressure gradient to activate fluid flow. Observation of fluid flow in both laboratory (Candela *et al.*, 2014) and field (Bonini, 2020) due to dynamic stresses provided compelling evidence that the numerically observed PS mechanism might be real. The question is: Can we see PS in the laboratory?

# **Laboratory Setup and Methods**

In this article, we performed lab experiments in a water tank (Fig. 1) to investigate whether PS exists in a fluid-filled fracture. We designed and built an experiment platform (Fig. 1a), including a new low-frequency source and new pressure sensor (P1, H1–H5 in Fig. 1b), to directly measure pressure changes. We submerged all components underwater during the experiment. The real picture of the whole low-frequency experiment platform submerged underwater is shown in Figure 2a. Designing the low-frequency seismic source and the new pressure sensor that can be placed in a thin fracture are two challenges.

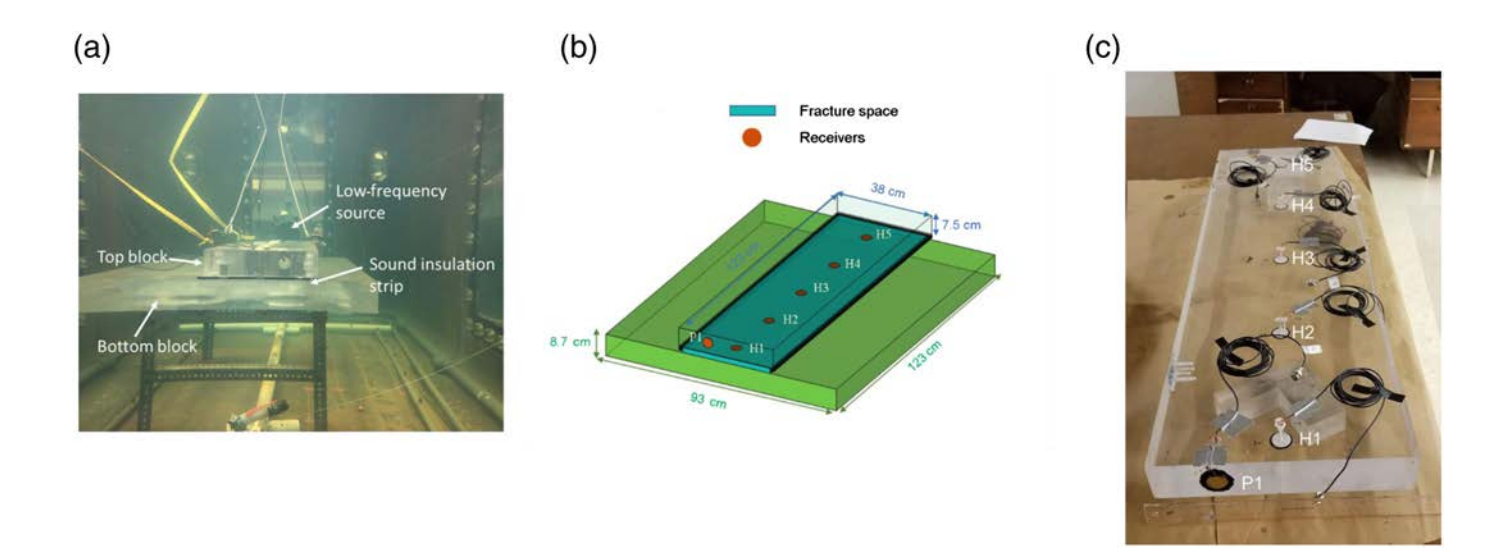
In the past, most physical modeling experiments in labs (Nakagawa *et al.*, 2016; Shih and Frehner, 2016) used ultrasonic frequencies of  $\sim 10^5 - 10^7$  Hz. Because the PS effect occurs only in the low-frequency regime (f < 100 Hz) (Zheng, 2018) for the materials we used, we could not use the commercially available high-frequency laboratory systems in our experiments. Our source is an electromagnetic acoustic source that

**Figure 1.** Experiment setup. (a) Schematic of the entire experiment platform in a water tank (box). The water tank is 4 m long, 1.9 m wide, and 1.5 m deep. The total water depth is 1.2 m. The water depth to the top of the fracture model is 0.7 m. The experiment platform contains three parts: a low-frequency acoustic source (circular gray object), a fracture model made by two acrylic glass blocks stacked on top of each other, and the six transducers measuring fluid pressure. (b) Schematic of the side view of the geometry. There are six pressure transducers (P1, H1–H5) installed on the fracture model. The horizontal distance from the source to P1 is 1.1 m.

can generate sinusoid waves from 12 to 70 Hz. The source amplitude can be controlled by a signal generator.

The fracture model was built from two plexiglass blocks stacked upon each other (Fig. 2b). We adjusted the fracture aperture by changing the thickness of the washers inserted between the blocks. Three sides of the fracture were sealed by the neoprene sound insulation strip to prevent fluid leakage. Only the front side facing the source was left open. Because the fluid in the fracture could freely move into the water tank from the front side, the observed pressure amplification in the fracture was not caused by the weight of the upper block. The fracture geometry was fixed during the experiment, and the pressure amplification did not further rupture the fracture.

To measure the fluid pressure inside the thin fracture (<10 mm) directly, we needed high-sensitivity sensors of small physical sizes. Commercially available hydrophones are too large in dimension to be put into a thin fracture. We custombuilt six transducers and installed them on the upper block (Fig. 2c). Our transducer design was similar to the flexural bender design (Lee *et al.*, 2010) that can record in the frequency range of 0.1–600 Hz. Five of them labeled, H1–H5, were installed inside the fracture and spaced at an equal distance to measure the fluid pressure. One transducer (P1) was



installed on the front façade of the top block but outside of the fracture, which measured the incident-wave amplitude.

To systematically characterize the PS effect, we need to compare the wave amplitudes measured in the fracture and the incident-wave amplitude measured outside the fracture. Therefore, we first calibrated the six transducers to the same sensitivity. We purchased the commercial scientific hydrophone AS-1 from Aquarian Audio company for calibration. AS-1 has a stable linearity response from 1 Hz to 100 kHz with a sensitivity  $-208 \text{ dBV}/1\mu\text{Pa}$ . The diameter of the AS-1 is 12 mm. We set up a calibration experiment for which schematic is shown in Figure 3a. The fracture aperture is set to 15.5 mm such that we can put the AS-1 hydrophone inside the fracture next to H1-H5. We used both our low-frequency sinusoid source and the airbubble source to calibrate the pressure sensors (H1-H5). In the bubble source cases, we blew air through a tube into the water tank to create bubbles to excite the acoustic waves. For both types of sources, we recorded the waveforms simultaneously using our transducer and the AS-1 hydrophones. A band-pass filter (3-150 Hz) was applied to the raw data to remove the shallow water wave and highlight the low-frequency signal of interest. Figure 3b,c shows comparison of recorded waveforms between our transducers and AS-1X (inside fracture) and AS-1F (outside the fracture) using our new low-frequency source. Figure 3d and 3e shows waveform comparison for two different sets of air bubbles, respectively. These tests (Fig. 3) showed that our transducers under both broadbands (bubbles), and our mono-frequency sources can be used to study the PS effect.

We conducted PS measurements for six different fracture apertures: 9.2, 4.7, 1.7, 0.95, 0.4, and 0.2 mm. Our low-frequency

**Figure 2.** Picture of the low-frequency platform. (a) Finished low-frequency experiment platform submerged in the water tank. (b) Fracture model and the locations of the six installed transducers (P1 and H1–H5). P1 is installed on the front facade of the top block. The other five (H1–H5) are in the fracture. The physical dimensions of the two blocks are labeled. The black line between the blocks is the seal material. (c) Real picture of the top block with our high-sensitivity transducers installed.

sinusoid source was set to vibrate at one frequency at a time, in the frequency range of 12–70 Hz, at every 1 Hz interval. For each experiment (frequency, aperture), we recorded 10 s of waveforms. We then band-pass filtered the recorded waveforms (passband: 3–150 Hz) and analyzed the PS effect.

# PS Results in the Time and Frequency Domains

We first show time-domain waveforms recorded by P1 and H1–H5 (Fig. 4) at two sinusoidal source frequencies, 35 and 29 Hz, for a fracture aperture of 0.95 mm. We use the waveform recorded by P1 as a proxy for the incident-wave amplitude. To quantify PS, we define a pressure surge factor (PSF) as the ratio of the spectral amplitude of Hn (n = 1, 2, 3, 4, 5) waveform to that of P1. At 35 Hz, we observe no obvious amplification for H1–H5 (Fig. 4). On the other hand, if the source frequency is 29 Hz, the recorded wave amplitudes of H1–H5 are greatly amplified compared with P1. In addition, PSF appears to vary within the fracture: H3 has the smallest PSF, H1 and H2 are intermediate, and H4 and H5 have the two largest PSFs (25.2 and 19.9, respectively). The drastic increase of wave amplitude at a certain frequency may imply

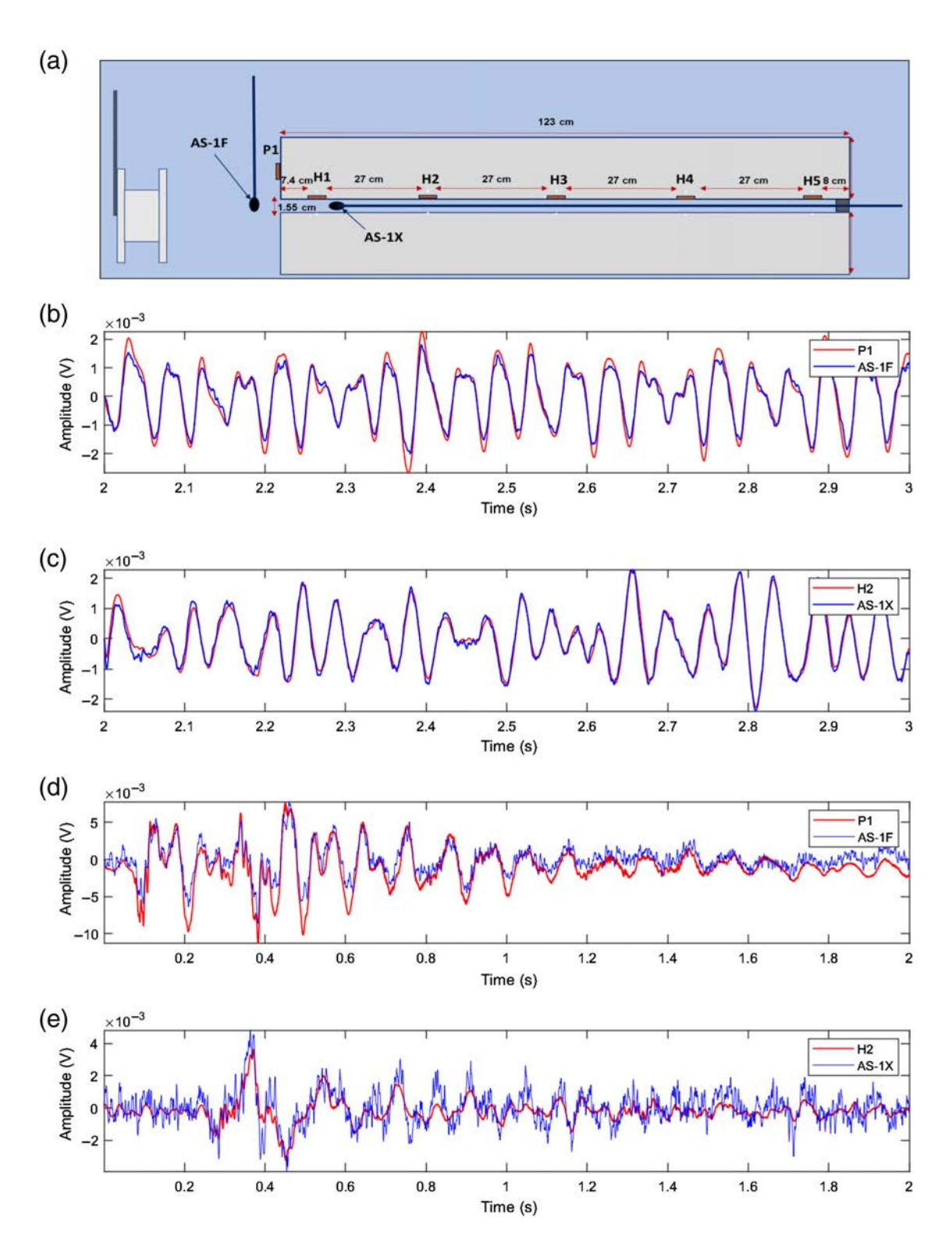


**Figure 3.** Pressure sensor calibration and benchmark test. AS-1F is the hydrophone placed in front of the fracture model. AS-1X is placed close to H1–H5 inside the fracture. (a) Source and receiver geometry. Here it shows our sinusoidal low-frequency source. For the broadband test, the sinusoidal low-frequency source is replaced by air bubbles. (b) Comparison between the calibrated P1 and AS-1F waveforms using

our low-frequency source (22 Hz). (c) Comparison between the calibrated H2 and AS-1X waveforms using our low-frequency source (22 Hz). (d) Comparison between the calibrated P1 and AS-1F waveforms using air-bubble source. (e) Comparison between the calibrated H2 and AS-1X using the air-bubble source.

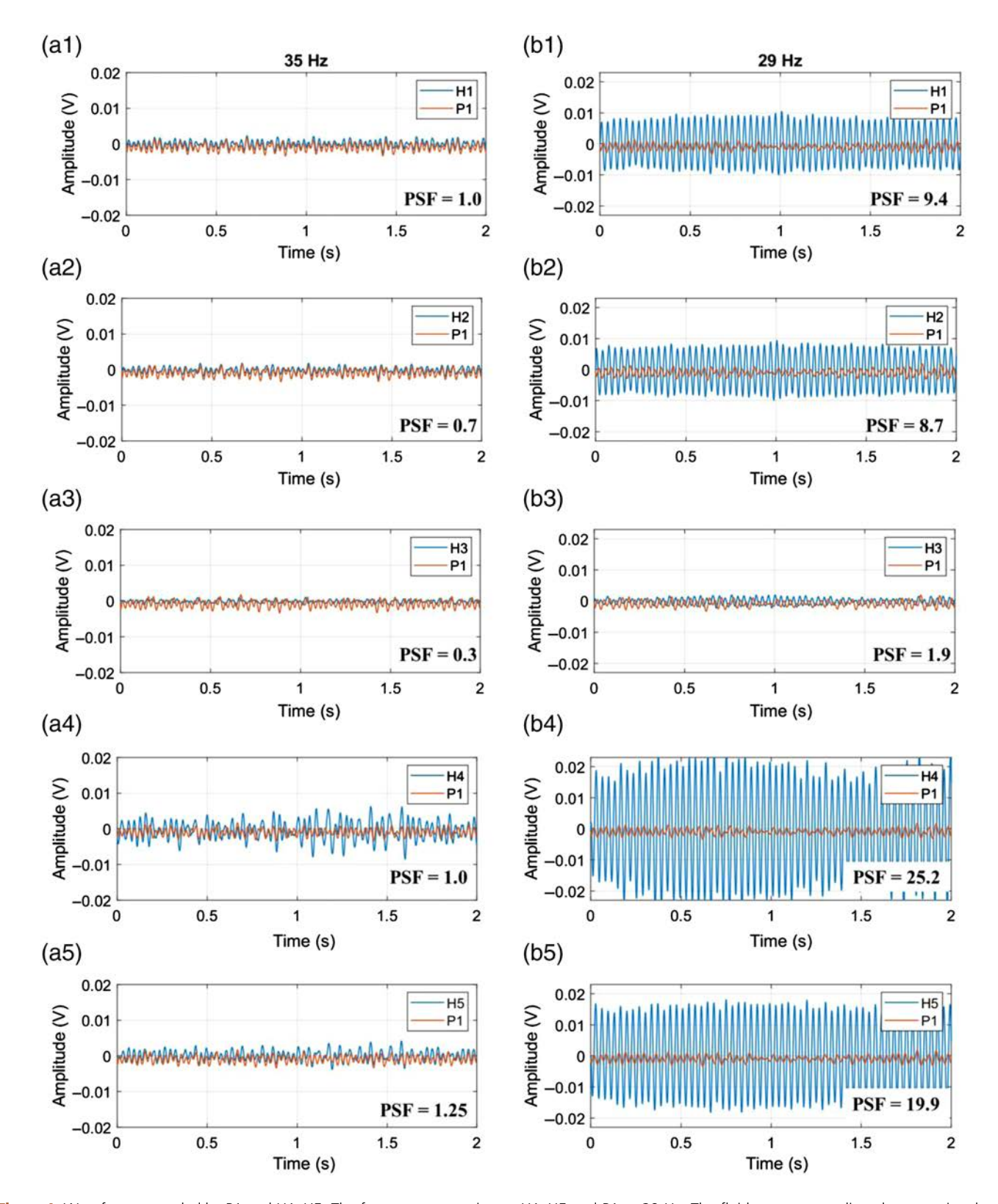
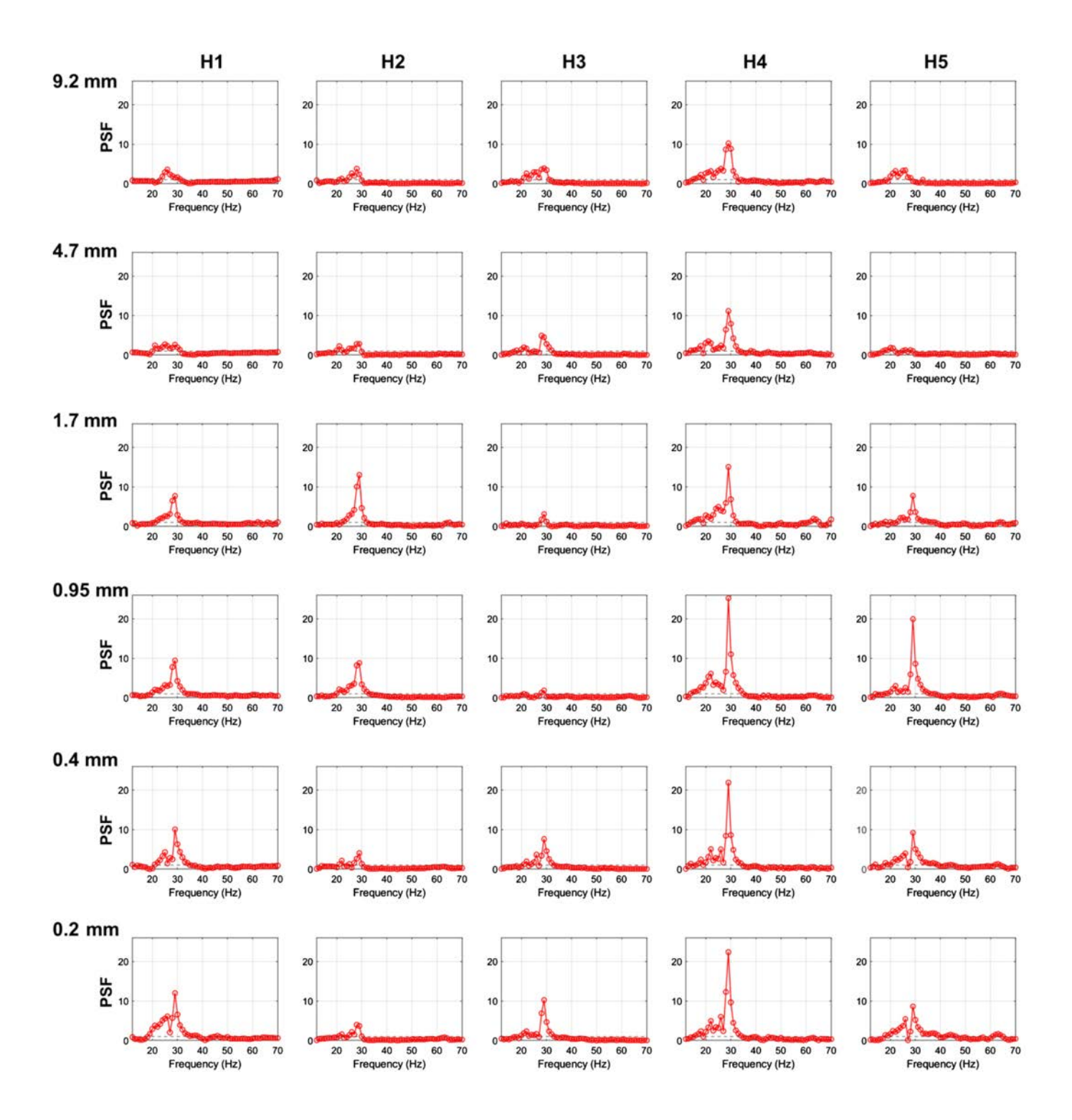


**Figure 4.** Waveforms recorded by P1 and H1–H5. The fracture aperture is 0.95 mm, and two source frequencies, 35 and 29 Hz, are used. The left panels, (a1)–(a5), show the waveforms measured in Volts by H1–H5 and P1 at 35 Hz. The right panels, (b1)–(b5), show the waveforms recorded by

H1–H5 and P1 at 29 Hz. The fluid pressure was linearly proportional to voltage. All waveform amplitudes are calibrated, so their magnitudes can be compared.



resonance caused by the Krauklis wave due to the fluid-filled fracture (Liang et al., 2020).

We also computed the frequency-domain PSF for the five receivers, H1–H5, and for six fracture apertures from 12 to 70 Hz. As a result, we have a total of 30 (=  $5 \times 6$ ) PSF curves as a function of frequency (Fig. 5). The maximum PSF (25.2)

**Figure 5.** Pressure surge factors (PSFs) at receivers H1–H5 (columns) for six different fracture apertures (rows) as a function of frequency.

occurs at H4 at a fracture aperture of 0.95 mm. The experiment results clearly verify the claim that the dynamic pressure in a fluid-filled fracture can be amplified relative to the incidentwave pressure. There are several salient features in Figure 5. The frequency of the highest PSF appears to be around 29 Hz for most of the 30 cases. For H1, the frequency location of the highest PSF peak shifts from 25 to 29 Hz, and the PSF monotonically increases from 3.3 to 12.0 with a decreasing aperture from 9.2 to 0.2 mm. Similarly, the highest PSF peak frequency shifts from 22 to 29 Hz for H5, and PSF increases from 3.6 to 19.9, as the aperture decreases from 9.5 to 0.95 mm. Furthermore, as the fracture aperture decreases from 9.2 to 0.95 mm, the PSF of H4 steadily increases from 10 to 25.2 —the highest PSF in all our experiments. Given the limitations of our experimental conditions, ambient noise might influence our results. When we turned off the source and measured the noise, the ambient noise was not able to cause PSF > 2.

#### Discussion

Our lab observations of transient PS in a fluid-filled fracture can have a range of implications and applications. First, the existence of PS needs presence of fluids and fractures. PS is consistent with the important role of fluid and fractures in earthquake dynamic triggering, in both extensional (Hill, 2008) and compressional (Wang et al., 2018) tectonic stress regimes. Second, PS is a frequency-dependent phenomenon. The frequency-dependent amplification explains why frequency is more important than the peak ground velocity in triggering natural earthquakes (Brodsky and Prejean, 2005; Aiken and Peng, 2014; Pankow and Kilb, 2020) and inducing seismicity in hydraulic-fracturing settings (Wang et al., 2018). In natural earthquake triggering, the triggering frequency (<1 Hz) is much lower than the frequency (~29 Hz) we obtained here. This discrepancy could be explained by the length scale difference between the lab fracture and the field fracture. According to the 2D numerical modeling (Zheng, 2018), for a 8 m long granite fracture filled with water with a 2 mm fracture aperture, PS can happen at <0.5 Hz. Tary, van der Baan, and Eaton (2014) and Tary, van der Baan, Sutherland, and Eaton (2014) observed discrete resonance frequencies (tens of Hz) in hydraulic stimulation and monitoring in Canada.

PS also provides a natural mechanism to elevate the fluidpore pressure abruptly, as the triggering wave passes by to trigger earthquakes. In the Coulomb failure (Kilb *et al.*, 2000; Hill, 2008), the shear stress,  $\tau$ , acting on the fault shall be greater than the resistance force,  $F = \mu(\sigma_n - p) + C$ , in which  $\mu$  is the coefficient of internal friction,  $\sigma_n$  is the normal stress in the rock, p is the fluid pressure, and C (nonnegative) is the cohesion of materials. Obviously, if p increases, F will decrease, so the failure criterion,  $|\tau| > F$ , is more likely to be met.

Because the perturbing stress level of the incident wave is extremely low (several kPa to tens of kPa), previous researchers thought that the pore pressure must be very close to (more than 99% of) the lithostatic pressure in locations of dynamic triggering (Brodsky and Prejean, 2005). This stringent requirement may be relaxed, if PS plays a role. For example, taking a typical incident stress ~0.1 MPa (Hill, 2008), a PSF of 25 can cause a fluid pressure change of ~2.5 MPa transiently. In reality, we might be able to achieve PSF > 100, if the fracture were longer and the corresponding amplification frequencies could be much lower (<0.5 Hz) (Zheng, 2018). Therefore, a sublithostatic pore pressure that is not close to the failure stress can still be amplified to cause the Coulomb failure to trigger earthquakes by PS. Zoback and Gorelick (2012) argue that large-scale geologic storage of carbon dioxide can cause earthquakes due to pore pressure increase to cause CO2 leakage. PS may exacerbate the situation.

From an observational point of view, precise determination of the frequencies of the triggering seismic waves coming from different directions can be used to constrain subsurface the fracture geometry and fracture hydraulic transmissivity. PS can also be used to understand how hydrogeological permeability changes are associated with seismic waves. PS causes localized pressure gradient to drive fluid flow that may unclog the fracture and cause the permeability changes observed both in laboratory experiments (Elkhoury *et al.*, 2011) and in the field (Manga *et al.*, 2012).

Although we clearly observe the PS effect in the lab, more experiments using larger fracture blocks of real rocks or even in the field are necessary to further explore this phenomenon. Future studies that use different fracture sizes will help us better understand these findings. We observed in many cases (Fig. 5) that the highest PSF value appears around 29 Hz, even for different fracture apertures. We used the dispersion equation (Korneev, 2008) to estimate the resonance frequency. The resonance frequency of our 0.95 mm aperture model is ~24 Hz, which is not exactly the same as our measured peak frequency but in a similar order of magnitude. A possible explanation for this frequency discrepancy could be that in 3D settings the resonance frequency might also be controlled by the length and width of the fracture, not just the aperture for this small-size model (Ferrazzini and Aki, 1987; Korneev et al.,

2014). If the width has a greater influence on the resonance, it is possible that peak frequency does not change much with aperture. This hypothesis should be verified by 3D numerical modeling in the future.

Our experiment results provide important evidence toward understanding the underlying mechanism in earthquake dynamic triggering. The transient PS effect can simultaneously address several robust observational aspects of the remote triggering: low-stress perturbation of the incident seismic waves, the frequency dependence, and the affinity to fluids. PS may also play a role in triggering near-field aftershocks in geothermal and volcanic regions observed notably after the Landers earthquake (Hill *et al.*, 1993; Kilb *et al.*, 2000). The observation of PS may not have solved the puzzle of dynamic earthquake triggering, but it seems to be an important step toward this goal.

#### Conclusions

We invented a low-frequency experimental platform that is able to excite low-frequency sinusoid waves in the frequency range of ~12–70 Hz and directly record fluid pressure in thin fractures using our newly custom-built transducers (~0.1–600 Hz). We have demonstrated in the lab that a fluid-filled fracture can indeed cause localized transient pressure amplification, which provides a plausible explanation for the dynamic earthquake triggering by the passage of seismic waves. The maximum observed PSF is 25.2 using our lab fracture model, and larger PSF could be obtained for larger fracture sizes. This newly observed transient PS phenomenon may also open a new research direction that can potentially present us with new opportunities to develop novel subsurface sensing techniques or control the hydraulic-fracturing process in unconventional and enhanced geothermal energy development.

#### **Data and Resources**

The data used in this article have been archived in the Texas Data Repository with doi: 10.18738/T8/T2BRGA. The link of the repository is https://dataverse.tdl.org/dataset.xhtml?persistentId =doi%3A10.18738%2FT8%2FT2BRGA (last accessed June 2021).

### **Declaration of Competing Interests**

The authors declare that there is no conflict of interest.

## Acknowledgments

The authors thank Ruijia Wang and Debi Kilb for helping review this article. They also appreciate the feedback given to them by Zhigang Peng, John Suppe, and Christine Ehlig-Economides. The authors also appreciate David Li for proof-reading the article for English and clarity. The authors thank the Allied Geophysical Laboratories (AGL) for allowing them to use the lab facilities. National Science Foundation (NSF) funds the work under the Funding Number EAR-1833058.

#### References

- Aiken, C., and Z. Peng (2014). Dynamic triggering of microearth-quakes in three geothermal/volcanic regions of California, *J. Geophys. Res.* **119**, no. 9, 6992–7009.
- Bonini, M. (2020). Investigating earthquake triggering of fluid seepage systems by dynamic and static stresses, *Earth Sci. Rev.* **210**, 103343, doi: 10.1016/j.earscirev.2020.103343.
- Brodsky, E. E., and S. G. Prejean (2005). New constraints on mechanisms of remotely triggered seismicity at Long Valley Caldera, *J. Geophys. Res.* **110**, no. B4, doi: 10.1029/2004JB003211.
- Brodsky, E. E., and N. J. van der Elst (2014). The uses of dynamic earthquake triggering, in *Annual Review of Earth and Planetary Sciences*, R. Jeanloz (Editor), Vol. 42, 317–339.
- Candela, T., E. E. Brodsky, C. Marone, and D. Elsworth (2014). Laboratory evidence for particle mobilization as a mechanism for permeability enhancement via dynamic stressing, *Earth Planet. Sci. Lett.* 392, 279–291.
- Cattania, C., J. J. McGuire, and J. A. Collins (2017). Dynamic triggering and earthquake swarms on East Pacific Rise transform faults, *Geophys. Res. Lett.* **44**, no. 2, 702–710.
- Elkhoury, J. E., A. Niemeijer, E. E. Brodsky, and C. Marone (2011). Laboratory observations of permeability enhancement by fluid pressure oscillation of in situ fractured rock, *J. Geophys. Res.* **116**, doi: 10.1029/2010JB007759.
- Ferrazzini, V., and K. Aki (1987). Slow waves trapped in a fluid-filled infinite crack—Implication for volcanic tremor, *J. Geophys. Res.* **92**, no. B9, 9215–9223.
- Hill, D. P. (2008). Dynamic stresses, coulomb failure, and remote triggering, *Bull. Seismol. Soc. Am.* **98**, no. 1, 66–92.
- Hill, D. P., and S. G. Prejean (2015). Dynamic triggering, in *Treatise on Geophysics*, G. Schubert (Editor), Vol. 4, Elsevier, Oxford, United Kingdom, 273–304.
- Hill, D. P., P. A. Reasenberg, A. Michael, W. J. Arabaz, G. Beroza, D. Brumbaugh, J. N. Brune, R. Castro, S. Davis, D. Depolo, et al. (1993). Seismicity remotely triggered by the magnitude 7.3 Landers, California, earthquake, Science 260, no. 5114, 1617–1623.
- Kilb, D., J. Gomberg, and P. Bodin (2000). Triggering of earthquake aftershocks by dynamic stresses, *Nature* **408**, no. 6812, 570–574.
- Korneev, V. (2008). Slow waves in fractures filled with viscous fluid, *Geophysics* **73**, no. 1, N1–N7.
- Korneev, V., L. Danilovskaya, S. Nakagawa, and G. Moridis (2014). Krauklis wave in a trilayer, *Geophysics* **79**, no. 4, L33–L39.
- Krauklis, P. V. (1962). About some low frequency oscillations of a liquid layer in elastic medium, *PMM* **26**, no. 6, 1111–1115 (in Russian).

- Lee, H., S. Choi, and W. Moon (2010). A micro-machined piezoelectric flexural-mode hydrophone with air backing: Benefit of air backing for enhancing sensitivity, J. Acoust. Soc. Am. 128, no. 3, 1033–1044.
- Li, C., Z. Peng, J. A. Chaput, J. I. Walter, and R. C. Aster (2021). Remote triggering of Icequakes at Mt. Erebus, Antarctica by large teleseismic earthquakes, *Seismol. Res. Lett.* doi: 10.1785/0220210027.
- Liang, C., L. Karlstrom, and E. M. Dunham (2020). Magma oscillations in a conduit-reservoir system, application to very long period (VLP) seismicity at basaltic volcanoes: 1. Theory, *J. Geophys. Res.* **125**, no. 1, doi: 10.1029/2019JB017437.
- Manga, M., I. Beresnev, E. E. Brodsky, J. E. Elkhoury, D. Elsworth, S. E. Ingebritsen, D. C. Mays, and C. Y. Wang (2012). Changes in permeability caused by transient stresses: Field observations, experiments, and mechanisms, *Rev. Geophys.* 50, doi: 10.1029/2011RG000382.
- Nakagawa, S., S. Nakashima, and V. A. Korneev (2016). Laboratory measurements of guided-wave propagation within a fluid-saturated fracture, *Geophys. Prospect.* **64**, no. 1, 143–156.
- Pankow, K. L., and D. Kilb (2020). Going beyond rate changes as the sole indicator for dynamic triggering of earthquakes, *Sci. Rep.* **10**, no. 1, 1–12.
- Peng, Z., C. Wu, and C. Aiken (2011). Delayed triggering of microearthquakes by multiple surface waves circling the Earth, *Geophys. Res. Lett.* **38**, doi: 10.1029/2010GL046373.
- Prejean, S. G., D. P. Hill, E. E. Brodsky, S. E. Hough, M. J. S. Johnston,S. D. Malone, D. H. Oppenheimer, A. M. Pitt, and K. B. Richards-Dinger (2004). Remotely triggered seismicity on the United States

- West Coast following the  $M_{\rm w}$  7.9 Denali Fault earthquake, *Bull. Seismol. Soc. Am.* **94**, no. 6B, S348–S359.
- Shih, P.-J. R., and M. Frehner (2016). Laboratory evidence for Krauklis-wave resonance in fractures and implications for seismic coda wave analysis, *Geophysics* **81**, no. 6, T285–T293.
- Tary, J. B., M. van der Baan, and D. W. Eaton (2014). Interpretation of resonance frequencies recorded during hydraulic fracturing treatments, J. Geophys. Res. 119, no. 2, 1295–1315.
- Tary, J. B., M. van der Baan, B. Sutherland, and D. W. Eaton (2014). Characteristics of fluid-induced resonances observed during microseismic monitoring, J. Geophys. Res. 119, no. 11, 8207–8222.
- Wang, B., R. M. Harrington, Y. Liu, H. Kao, and H. Yu (2018). Remote dynamic triggering of earthquakes in three unconventional Canadian hydrocarbon regions based on a multiple-station matched-filter approach, *Bull. Seismol. Soc. Am.* 109, no. 1, 372–386.
- Zheng, Y. (2018). Transient pressure surge in a fluid-filled fracture. Short note, *Bull. Seismol. Soc. Am.* **108**, no. 3A, 1481–1488.
- Zoback, M. D., and S. M. Gorelick (2012). Earthquake triggering and large-scale geologic storage of carbon dioxide, *Proc. Natl. Acad. Sci. Unit. States Am.* **109**, no. 26, 10,164–10,168.
- Zoback, M. D., and M. L. Zoback (2002). State of stress in the Earth's lithosphere, in *International Handbook of Earthquake and Engineering Seismology, Part A*, W. Lee, H. Kanamori, P. C. Jennings, and C. Kisslinger (Editors), Academic Press, Amsterdam, The Netherlands, 559–568.

Manuscript received 4 May 2021
Published online 6 July 2021